## **ORGANOMETALLICS**

pubs.acs.org/Organometallics Article

## **Borataalkene Hydrofunctionalization Reactions**

Tyler A. Bartholome, Jesse J. Martinez, Aishvaryadeep Kaur, David J. D. Wilson, Jason L. Dutton, and Caleb D. Martin\*



**Cite This:** *Organometallics* 2021, 40, 1966–1973



**ACCESS** 

III Metrics & More

Article Recommendations

s Supporting Information

**ABSTRACT:** The hydrofunctionalization of alkenes is a foundational class of reactions; however, the analogous reactions for B=C bond-containing species have been virtually unexplored. This work unearths a range of B=C hydrofunctionalization reactions with the 9-borataphenanthrene anion, including hydroalkylation, hydroarylation, hydroalkynylation, hydroamination, hydroalkoxylation, and hydration. The unique reactivity represents an addition to the synthetic chemist's toolbox to access functionalized tetracoordinate borates.

$$\mathsf{R}^{\mathsf{S}} = \mathsf{1}; \, \mathsf{R} = \mathsf{CH}_2\mathsf{CN}, \\ \mathsf{CgF}_5, \, \mathsf{CCPh}, \, \mathsf{NPh}_2 \\ \mathsf{Hydrofunctionalization} \\ \mathsf{R} = \mathsf{1}; \, \mathsf{R} = \mathsf{CH}_2\mathsf{CN}, \\ \mathsf{NPh}_2 \\ \mathsf{Hydrofunctionalization} \\ \mathsf{R} = \mathsf{1}; \, \mathsf{R} = \mathsf{CH}_2\mathsf{CN}, \\ \mathsf{NPh}_2 \\ \mathsf{NPh}_3 \\ \mathsf{NPh}_4 \\ \mathsf{NPh}_4 \\ \mathsf{NPh}_4 \\ \mathsf{NPh}_4 \\ \mathsf{NPh}_5 \\ \mathsf{NPh}_6 \\ \mathsf{NPh}_$$

## ■ INTRODUCTION

Hydrofunctionalization reactions of alkenes are a valuable synthetic tool and, accordingly, have been studied extensively in recent decades.<sup>1–7</sup> This class of reactions consists of the addition of an element—hydrogen bond across a carbon—carbon double bond (Scheme 1). Prominent examples of

Scheme 1. Hydrofunctionalization Reactions of an Olefin with an  $\alpha$ -Olefin as an Example

$$= R + E-H \longrightarrow H E or E H$$

$$R = BR_2, CR_3, NR_2, OR$$

hydrofunctionalization reactions for olefins include hydroboration, <sup>5,8-14</sup> hydrosilylation, <sup>5,13,15-18</sup> hydroamination, <sup>19-22</sup> hydroalkoxylation, <sup>23,24</sup> and hydrocarbonation. <sup>7,15,25-35</sup> Intriguingly, some examples of hydrofunctionalization reactions, specifically hydroboration, hydrophosphination, and hydroamination, have recently been realized for boron—boron double and triple bonds by Braunschweig and co-workers. <sup>36-40</sup>

Borataalkenes, anionic boron-containing analogues of olefins, have been known since 1972 and, although somewhat rare, 41,42 have been demonstrated to undergo a variety of transformations, 43-45 including alkylation at carbon, 43,46,47 epoxide ring opening, 48,49 and the "boron-Wittig" reaction. 43,50-52 Despite the abundance of literature on olefin hydrofunctionalization, the hydrofunctionalization reactivity of borataalkenes has remained largely unexplored. The Erker and Yamashita groups have demonstrated that zwitterionic borataalkenes react with hydroboranes to form species containing four-membered BHBC rings (Scheme 2). 53-56 The anionic borataalkene moiety of 9-borataphenanthrene anion A undergoes hydroboration with pinacolborane (HBpin) to produce a tetracoordinate boron species in which the

Scheme 2. Selected Examples of Reactions of Borataalkene-Containing Species with Hydroboranes<sup>a</sup>

Erker, 2015: 
$$C_6F_5$$
 $PHMes_2$ 

Yamashita, 2020:

 $Et_2N^{\oplus}=C=C=BR_2$ 
 $R_2$ 
 $R_2$ 
 $R_2$ 
 $R_3$ 
 $R_4$ 
 $R_2$ 

Martin, 2020:

 $R_4$ 
 $R_2$ 
 $R_4$ 
 $R_4$ 
 $R_5$ 
 $R_4$ 
 $R_5$ 
 $R_5$ 
 $R_5$ 
 $R_5$ 
 $R_5$ 
 $R_5$ 
 $R_5$ 
 $R_5$ 
 $R_6$ 
 $R_7$ 
 $R_8$ 
 $R_8$ 
 $R_8$ 
 $R_8$ 

Martin, 2020:

 $^a\mathrm{Mes} = 2,4,6$ -trimethylphenyl, BR $_2 = 9$ -borabicyclo[3.3.1]nonyl, pin = pinacolate.

hydride is not bridged between the two boron centers.<sup>57</sup> Aside from the aforementioned hydroboration reactivity, examples of borataalkene hydrofunctionalization reactions are generally absent from the literature.<sup>58</sup> Given the vast utility of alkene hydrofunctionalization chemistry and limited precedent for

Received: April 28, 2021 Published: June 11, 2021





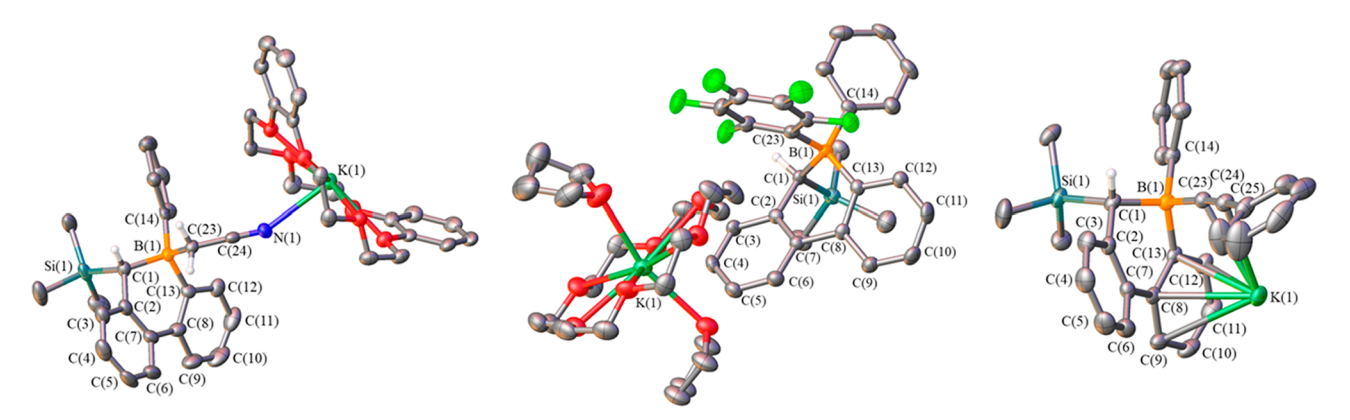


Figure 1. Solid-state structures of 1, 2, and 3 (left to right). Hydrogen atoms (except those from the C-H addition event) and noncoordinated solvates are omitted for clarity, and thermal ellipsoids are drawn at the 50% probability level. For disordered atoms, only the component with the higher occupancy is shown. Only the asymmetric unit is displayed for 3; the full dimeric structure is shown in the SI (Figure S-36).

B=C bond hydrofunctionalization, we herein investigate the potential of a B=C system for hydrofunctionalization reactivity.

## ■ RESULTS AND DISCUSSION

Addition reactions of C-H bonds across unactivated olefins are generally challenging transformations. 3,26,30,31 However, given that the polarization of the B=C bond results in an electron-rich carbon center, we envisioned that a borataalkene might engage in C-H bond addition reactivity. The reaction of A with neat acetonitrile at room temperature led to a new singlet in the tetracoordinate region at -12.8 ppm in the in situ <sup>11</sup>B NMR spectrum after 4 days (cf. A = 40.4 ppm). Complete conversion could be achieved upon heating at 80 °C for 16 h. Sequestration of the potassium countercation with dibenzo-18crown-6 enabled isolation in 66% yield of the major product, determined by X-ray crystallography to be the cyanomethylsubstituted tetracoordinate boron species 1 (Figure 1). Syn addition of an acetonitrile C-H bond across the borataalkene B=C bond occurred rather than insertion of the cyano group into the C-Si bond of A (Scheme 3). This differs from nitrile/ silyl carbanion reactivity observed for trimethylsilyl-substituted alkyllithium reagents, which undergo cyano group insertion

Scheme 3. C—H Activation Reactivity of A with Acetonitrile, Pentafluorobenzene, and Phenylacetylene<sup>a</sup>

into the C–Si bond to produce *N*-trimethylsilyl-1-azaallyl anions. <sup>59,60</sup> The <sup>1</sup>H NMR spectrum of 1 contains three signals integrating in a 1:1:1 ratio for the three aliphatic protons derived from acetonitrile: a singlet at 1.19 ppm assigned to the proton added to the borataalkene carbon and two multiplets at 1.31–1.27 ppm and 1.02–0.98 ppm assigned to the two diastereotopic protons of the cyanomethyl group. An absorption band at 2212 cm<sup>-1</sup> in the FT-IR spectrum confirms the presence of the pendant nitrile.

Given the unusual C-H bond activation with acetonitrile (sp<sup>3</sup> C-H substrate), the activation of sp<sup>2</sup> and sp C-H bonds was targeted using pentafluorobenzene and phenylacetylene, respectively (Scheme 3). The reactions of A with excess pentafluorobenzene and phenylacetylene were monitored by in situ 11B NMR spectroscopy and resulted in complete consumption of A within 2 days at 60 °C for both reactions with signals in the tetracoordinate region observed at -9.7ppm (2) and -15.4 ppm (3), respectively. Compound 2 was isolated as the [K(18-crown-6)]+ salt in 45% yield, and 3 was isolated as the free potassium salt in 84% yield. 61 Single-crystal X-ray diffraction studies identified both species as the syn C-H addition products 2 and 3 for pentafluorobenzene and phenylacetylene, respectively (Figure 1). Aliphatic singlets at 2.23 and 1.42 ppm corresponding to the protonated borataalkene carbon were observed in the <sup>1</sup>H NMR spectra of 2 and 3, respectively. The reactivity of A with phenylacetylene differs from that of a tantalum-bound  $\eta^2$ borataalkene ligand, which underwent cyclization with the alkyne moiety of phenylacetylene to form a five-membered BC<sub>3</sub>Ta ring.

The uncatalyzed series of sp³, sp², and sp regioselective C– H addition reactivity is noteworthy and suggests that the borataphenanthrene B=C bond could react with other element—hydrogen bonds. Accordingly, we examined the reactivity of A with N–H and O–H bond-containing substrates. The reaction of A with excess diphenylamine at room temperature in THF resulted in complete conversion after 24 h to a tetracoordinate boron-containing product as indicated by *in situ* <sup>11</sup>B NMR spectroscopy ( $\delta$  = -4.1 ppm, Scheme 4). The product was isolated in 58% yield and identified as the *syn* hydroamination product 4 by a single-crystal X-ray diffraction study (Figure 2). A diagnostic aliphatic singlet at 2.05 ppm in the <sup>1</sup>H NMR spectrum was assigned as the proton derived from the N–H unit in diphenylamine, further confirming hydroamination of the B=C bond.

<sup>&</sup>lt;sup>a</sup>Relative stereochemistry depicted.

# Scheme 4. Reactions of A with N-H- and O-H-Containing Substrates<sup>a</sup>

<sup>a</sup>Relative stereochemistry depicted.

The reaction of A with phenol resulted in a different outcome than the N-H and C-H substrates. In this case, the 1:1 stoichiometric reaction did not result in an isolable product, but heating a 2:1 mixture at 60 °C for 24 h generated a single product exhibiting a tetracoordinate <sup>11</sup>B NMR signal at -1.5 ppm. X-ray crystallography revealed that, in addition to hydroalkoxylation of the borataalkene B=C bond, desilylation at the borataalkene carbon also occurred with the elimination of phenyl trimethylsilyl ether (5, Scheme 4, Figure 2). This structural assignment was corroborated by the absence of a trimethylsilyl singlet in the product <sup>1</sup>H NMR spectrum and the presence of two aliphatic multiplets at 2.11-2.07 ppm and 2.00-1.96 ppm corresponding to the diastereotopic protons at the 10-position. Additionally, generation of phenyl trimethylsilyl ether was indicated by the presence of a trimethylsilyl singlet ( $\delta = 0.16$  ppm in  $C_6D_6$ ) in the crude <sup>1</sup>H NMR spectrum. The reactivity of A with O-H-containing substrates was explored further by exposing a THF solution of A to water. This resulted in hydration of the B=C bond and hydrolysis of the C-Si bond with the elimination of trimethylsilanol (6, Scheme 4), similar to the reaction with phenol. Although this species could not be cleanly isolated, X-ray crystallography confirmed its generation (Figure 2).

The mechanism for the hydrofunctionalization reactivity of **A** with the various substrates was investigated using density functional theory (DFT) calculations for two different pathways (Scheme 5): one in which a simple addition event

occurs (observed for 1-4), and another that includes desilylation (observed for 5 and 6). In the formation of 1-4, the first step consists of deprotonation of the substrate by the borataalkene carbon to produce a 9,10-dihydro-9-boraphenanthrene (Int1). This is consistent with the Hirshfeld charge of -0.25 at carbon versus -0.08 at boron. The barrier for this step (TS1) was found to be higher for the three C-H addition reactions (120.2, 111.0, and 108.7 kJ/mol for acetonitrile, pentafluorobenzene, and phenylacetylene, respectively) than for the hydroamination with diphenylamine (82.2 kJ/mol). The difference in barrier height is consistent with the experimental observation that the hydroamination proceeds to completion at room temperature, while the three C-H activation reactions require elevated temperatures. The second step consists of coordination of the deprotonated substrate to the Lewis acidic boron center of Int1. Although a transition state could not be located for this step, a scan of the reaction energy surface with constrained geometry optimizations at a series of fixed B-C<sub>substrate</sub> bond distances (CH<sub>3</sub>CN substrate reaction) indicates that product formation may be considered a barrierless process (without a transition state), while the loss of planarity around the boron atom (from sp<sup>2</sup> to sp<sup>3</sup>) occurs very late on the reaction energy surface and requires minimal energy change. For all four substrates, formation of the B=C hydrofunctionalization product Prod1 was found to be thermodynamically favorable (Table 1).

For the formation of 5 and 6, protonation of the borataalkene carbon initially occurs as in the formation of 1-4, with barrier heights of 48.2 and 86.5 kJ/mol (consistent with the observed room-temperature reactivity) for the reactions with phenol and water, respectively. Although modeling the H<sub>2</sub>O reaction with a single H<sub>2</sub>O molecule was problematic, addition of an explicit water solvent molecule in the form of a water dimer (H2O-H2O) yielded more appropriate transition state and minimum energy structures. Following the formation of protonated borataphenanthrene Int1, however, nucleophilic attack by the deprotonated substrate occurs at silicon rather than boron. The electrophilicity at silicon is corroborated by a Hirshfeld charge of +0.38, which is considerably greater than that of boron at +0.11 in Int1. Desilylation subsequently produces the Cunsubstituted 9-borataphenanthrene anion Int2. Hydrofunctionalization of the B=C bond in Int2 then occurs in a manner analogous with that observed for A in the mechanism for the formation of 1-4 by deprotonation of the substrate by

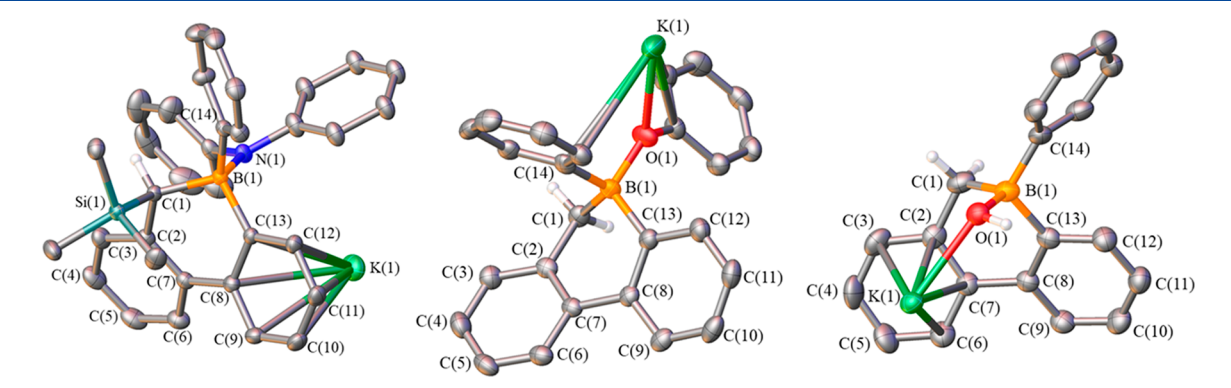


Figure 2. Solid-state structures of 4, 5, and 6 (left to right). Hydrogen atoms (except those derived from N–H or O–H bonds) and solvates are omitted for clarity. Thermal ellipsoids are drawn at the 50% probability level. Only the asymmetric units are displayed; the full polymeric structures are shown in the SI (Figures S-37, S-38, and S-39). For disordered atoms, only the component with the higher occupancy is shown.

Scheme 5. General Reaction Pathways Modeled for Hydrofunctionalization Reactions with A

Table 1. Calculated Reaction Free Energies ( $\Delta G$ , kJ/mol) for Pathways Arising from Proton Abstraction of the Substrate by A, Together with Experimental p $K_a$  (DMSO) of Substrates<sup>a</sup>

substrate	$pK_a^b$	TS1	Intl	Prod1	TS2	Int2	TS3	Int3	Prod2
$H_2O$	31.4	86.5	55.6	-47.3	103.6	-106.3	14.1	-9.7	-143.3
CH <sub>3</sub> CN	31.3	120.2	55.6	-11.2	151.1	-27.0	103.4	69.6	-25.7
$C_6F_5H$	29.0	111.0	37.2	-10.0	160.4	-27.0	100.0	51.2	-34.6
PhCCH	28.8	108.7	33.8	-52.2	123.0	-70.7	44.9	4.1	-113.5
$Ph_2NH$	25.0	82.2	21.9	-10.6	161.2	-58.6	26.0	4.4	-60.3
PhOH	18.0	48.2	-16.7	-71.6	64.3	-117.0	-70.6	-92.5	-171.2

"B3LYP-D3(BJ)/def2-TZVP(THF)//B3LYP-D3(BJ)/def2-SVP(THF) results, with energies given relative to the reactants.  $H_2O$  modeled as a hydrogen-bonded dimer  $H_2O-H_2O$ .  $^bpK_a$  in DMSO.  $^{64-69}$ 

the borataalkene carbon to produce 9,10-dihydro-9-boraphenanthrene Int3, which subsequently undergoes nucleophilic attack by the deprotonated substrate to form Prod2 in a barrierless process.

Further analysis of the desilylation pathway indicated that the formation of Prod2 is more thermodynamically favorable than the formation of Prod1 for all six substrates examined. This, combined with the large positive Hirshfeld charge at silicon in Int1, suggests that the system is kinetically controlled. Evidence supporting kinetic control is found when the barrier heights for TS2 and TS3 are compared with that of TS1 across all six reactions. For the three C-H substrates, the largest barrier is associated with TS3, which is greater than the TS1 barrier by 10.3, 16.1, and 6.8 kJ/mol for CH<sub>3</sub>CN, C<sub>6</sub>F<sub>5</sub>H, and PhCCH, respectively. With Ph<sub>2</sub>NH, the largest barrier is for TS2 (139.3 kJ/mol), which is 57.1 kJ/mol larger than for TS1. In contrast, the largest barrier on the Prod2 pathway for phenol (TS2, 80.9 kJ/mol) is smaller in magnitude than the TS1 barrier for PhCCH and C<sub>6</sub>F<sub>5</sub>H, which is consistent with PhOH forming Prod2 despite the fact that PhCCH and C<sub>6</sub>F<sub>5</sub>H form **Prod1** under similar experimental conditions. For water, the calculated barrier for TS3 of 120.5 kJ/mol is larger than for TS1 (86.5 kJ/mol), although the TS3 barrier is at the top of the range of barriers that can be crossed

at room temperature. Comparison of the  $pK_a$  of the substrate (Table 1) with the TS1 barrier height indicates a near-perfect linear relationship ( $r^2 = 0.992$  excluding  $H_2O$ , Figure S-40), which confirms the importance of the acidic proton character of the substrate. Water is an outlier to this trend, with a lower barrier than expected from the relationship to  $pK_a$  in DMSO, with the caveat that the  $pK_a$  of water varies widely depending on solvent. Since water does not follow the trend for TS1 barriers, it is possible that similar factors influence the TS2 and TS3 barrier heights, with the true barrier potentially being lower in energy. Modeling the system with larger water clusters could alter the calculated energetics; however, the results presented here for a water dimer provide qualitative agreement with experiment.

## CONCLUSION

The borataalkene moiety at the 9- and 10-positions of the 9-borataphenanthrene anion was demonstrated to undergo a variety of hydrofunctionalization reactions, including hydroalkylation, hydroarylation, hydroalkynylation, hydroamination, hydroalkoxylation, and hydration. Such hydrofunctionalization reactions were previously unexplored for borataalkenes, which is surprising given the extensively studied hydrofunctionalization reactivity of alkenes. The ability of the anionic B—C bond

to undergo diverse hydrofunctionalization reactivity presents B=C hydrofunctionalization as a potentially promising technique for the synthesis of tetracoordinate borates.

## **■ EXPERIMENTAL SECTION**

General Considerations. All manipulations were performed under an inert atmosphere in a nitrogen-filled MBraun Unilab glovebox or using standard Schlenk techniques. CD<sub>3</sub>CN and CDCl<sub>3</sub> for NMR spectroscopy were purchased from Cambridge Isotope Laboratories and dried by stirring for 3 days over CaH2, distilling, and storing over molecular sieves. THF-d<sub>8</sub> for NMR spectroscopy was purchased from Cambridge Isotope Laboratories and stored over molecular sieves. All other solvents were purchased from commercial sources as anhydrous grade, dried further using a JC Meyer Solvent System with dual columns packed with solvent-appropriate drying agents, and stored over molecular sieves. Compound A was prepared by the literature procedure.<sup>57</sup> The following reagents were purchased from the listed manufacturers and used as received: dibenzo-18crown-6 (TCI), pentafluorobenzene (TCI), 18-crown-6 (Oakwood Chemical), phenol (Sigma-Aldrich), and diphenylamine (Alfa Aesar). Phenylacetylene was purchased from Chem-Impex International and stored over molecular sieves. Multinuclear NMR spectra (1H, 13C-{1H}, 11B, 19F{1H}) were recorded on a Bruker Ascend 400 MHz instrument. High resolution mass spectra (HRMS) were obtained at the Baylor University Mass Spectrometry Center on a Thermo Scientific LTQ Orbitrap Discovery spectrometer using ESI. Melting points were measured with a Thomas-Hoover Unimelt capillary melting point apparatus and are uncorrected. FT-IR spectra were recorded on a Bruker Alpha ATR FT-IR spectrometer on solid samples. Single-crystal X-ray diffraction data were collected on a Bruker Apex II-CCD detector using Mo–K $\alpha$  radiation ( $\lambda$  = 0.71073 Å). Crystals were selected under paratone oil, mounted on MiTeGen micromounts, and immediately placed in a cold stream of N<sub>2</sub>. Structures were solved and refined using SHELXTL, and figures were produced using OLEX2.70,7

Computational Methods. Geometry optimization of reactants, products, intermediates, and TS structures was carried out at the B3LYP-D3(BJ) (refs 72–76)/def2-SVP (ref 77) level of theory inclusive of solvation (SMD model, Retrahydrofuran solvent). Frequency calculations were also performed analytically at the same level of theory to characterize all stationary points and to calculate thermodynamic corrections. Subsequent electronic energy calculations were carried out at the B3LYP-D3(BJ) (refs 72–76)/def2-TZVP (ref 77) (SMD model, Retrahydrofuran solvent) level. Extended Hirshfeld method CMS partial charges were calculated at the B3LYP-D3(BJ) (refs 72–76)/def2-TZVP (ref 77) (SMD model, Retrahydrofuran solvent) level. Single point calculations with wB97X-D (ref 81)/def2-TZVP (ref 77) (SMD model, Retrahydrofuran solvent) were also carried out and yielded equivalent results. All calculations were carried out in Gaussian 16.

Synthesis of 1. A (74 mg, 0.20 mmol) was dissolved in acetonitrile (3 mL) and heated to 80 °C in a pressure tube with a Teflon cap. After 16 h of heating, the volatile components were removed from the solution in vacuo, and the resulting pale yellow oil was redissolved in toluene (2 mL). A solution of dibenzo-18-crown-6 (74 mg, 0.20 mmol) in dichloromethane (2 mL) was then added to the product solution while stirring at room temperature. After an additional 30 min of stirring, the volatile components were removed from the solution in vacuo, and the residue was washed with toluene (10 mL) and dried in vacuo to yield 1 as a white powder. Yield: 103 mg (66%). d.p. 173 °C. Crystals for X-ray diffraction studies were grown by vapor diffusion of n-pentane into a 1,4-dioxane solution of 1. <sup>1</sup>H NMR (400 MHz, CD<sub>3</sub>CN):  $\delta$  7.68 (d, J = 7.0 Hz, 2H), 7.64– 7.60 (m, 2H), 7.57-7.55 (m, 1H), 7.17-7.14 (m, 2H), 7.10-7.05 (m, 2H), 7.03-6.99 (m, 1H), 6.97-6.95 (m, 10H), 6.94-6.90 (m, 1H), 4.17-4.15 (m, 8H), 3.94-3.92 (m, 8H), 1.31-1.27 (m, 1H), 1.19 (s, 1H), 1.02-0.98 (m, 1H), -0.75 (s, 9H);  $^{13}C\{^{1}H\}$  NMR (101 MHz, CD<sub>3</sub>CN): δ 149.21, 147.86, 142.81, 138.51, 135.48, 134.27, 132.03, 128.66, 127.12, 125.84, 125.81, 125.71, 125.07, 123.97,

123.31, 123.27, 122.33, 112.31, 70.03, 68.03, 0.53;  $^{11}\mathrm{B}$  NMR (128 MHz, CD<sub>3</sub>CN):  $\delta$  –12.8; FT-IR (cm $^{-1}$  (ranked intensity)): 2212 (14), 1504 (6), 1455 (10), 1247 (2), 1213 (4), 1120 (3), 1052 (7), 942 (5), 908 (11), 854 (8), 779 (15), 739 (1), 705 (9), 603 (12), 466 (13); high-resolution mass spectrometry (HRMS) electrospray ionization (ESI): calcd for C<sub>24</sub>H<sub>25</sub>BNSi [M] $^-$ , 366.1849; found, 366.1864.

Synthesis of 2. Pentafluorobenzene (0.423 mL, 3.81 mmol) was added to a solution of A (278 mg, 0.762 mmol) in THF (5 mL) while stirring at room temperature. The resulting solution was then transferred to a pressure tube with a Teflon cap and heated at 60 °C for 2 d, after which the solution was cooled to room temperature and filtered. A solution of 18-crown-6 (211 mg, 0.799 mmol) in THF (2 mL) was then added to the solution while stirring at room temperature. After 30 min of stirring, the volatile components were removed in vacuo to produce a red-orange oil, which was washed with 1:1 THF/n-pentane (5 mL) at -35 °C and dried in vacuo to yield 2 as a yellow-orange solid. Yield: 273 mg (45%). d.p. 78 °C. Crystals for X-ray diffraction studies were grown by storing the crude product oil at -35 °C. <sup>1</sup>H NMR (400 MHz, CDCl<sub>3</sub>):  $\delta$  7.93 (d, I = 7.0 Hz, 1H), 7.65 (d, J = 7.0 Hz, 2H), 7.51 (d, J = 7.0 Hz, 1H), 7.41 (d, J = 7.0 Hz, 1H), 7.15-7.05 (m, 5H), 7.00-6.97 (m, 1H), 6.91-6.82 (m, 2H), 3.48 (s, 24H), 2.23 (s, 1H), -0.63 (s, 9H); <sup>13</sup>C{<sup>1</sup>H} NMR (101 MHz,  $CDCl_3$ ):  $\delta$  150.69, 143.07, 138.87, 135.29, 134.04, 133.99, 133.95, 130.07, 125.98, 124.59, 124.21, 123.86, 123.26, 122.81, 121.47, 70.09, 1.03; <sup>11</sup>B NMR (128 MHz, CDCl<sub>3</sub>):  $\delta$  –9.7; <sup>19</sup>F{<sup>1</sup>H} NMR (376 MHz, CDCl<sub>3</sub>):  $\delta$  -129.64 (d, br, J = 1728 Hz, 2F), -166.42 (t, J = 20.5 Hz, 1F), -167.70-167.87 (m, 2F); FT-IR (cm<sup>-1</sup> (ranked intensity)): 2886 (12), 1503 (11), 1434 (3), 1350 (6), 1240 (8), 1104 (1), 1067 (10), 960 (2), 829 (4), 746 (5), 708 (7), 678 (13), 650 (14), 607 (9), 471 (15); high-resolution mass spectrometry (HRMS) electrospray ionization (ESI): calcd for C<sub>28</sub>H<sub>23</sub>BF<sub>5</sub>Si [M]<sup>-</sup>, 493.1582; found, 493.1539.

**Synthesis of 3.** Phenylacetylene (33  $\mu$ L, 0.30 mmol) was added to a solution of A (101 mg, 0.276 mmol) in THF (5 mL) while stirring at room temperature. The resulting solution was then transferred to a pressure tube with a Teflon cap and heated at 60 °C for 2 d, after which the volatile components were removed in vacuo to produce a yellow oil. The oil was then washed with benzene (5 mL) to produce a white precipitate, which was dried in vacuo to yield 3 as a white powder. Yield: 108 mg (84%). d.p. 114 °C. Crystals for X-ray diffraction studies were grown by storing a dichloromethane solution of 3 at -35 °C. <sup>1</sup>H NMR (400 MHz, CD<sub>3</sub>CN):  $\delta$  7.85 (d, J = 7.0 Hz, 2H), 7.62-7.59 (m, 1H), 7.56-7.52 (m, 1H), 7.50-7.49 (m, 1H), 7.15-6.90 (m, 13H), 1.42 (s, 1H), -0.70 (s, 9H);  ${}^{13}C\{{}^{1}H\}$  NMR (101 MHz, CD<sub>3</sub>CN):  $\delta$  150.34, 143.47, 136.40, 133.66, 131.76, 131.51, 129.66, 129.55, 128.76, 126.78, 125.97, 125.88, 124.84, 123.80, 123.31, 122.98, 0.76;  $^{11}$ B NMR (128 MHz, CD<sub>3</sub>CN):  $\delta$ -15.4; FT-IR (cm<sup>-1</sup> (ranked intensity)): 1593 (13), 1485 (8), 1425 (7), 1240 (3), 1054 (10), 897 (15), 828 (2), 741 (1), 712 (5), 692 (12), 676 (4), 613 (6), 578 (14), 529 (9), 466 (11); high-resolution mass spectrometry (HRMS) electrospray ionization (ESI): calcd for

C<sub>30</sub>H<sub>28</sub>BSi [M]<sup>-</sup>, 427.2053; found, 427.2071. **Synthesis of 4.** A solution of diphenylamine (171 mg, 1.01 mmol) in THF (2 mL) was added to a solution of A (74 mg, 0.20 mmol) in THF (2 mL) while stirring at room temperature. After 24 h of stirring, the volatile components were removed in vacuo to produce a yellow oil, which was lyophilized from benzene (3 mL) and washed with *n*-pentane (8  $\times$  10 mL) to yield 4 as a yellow powder. Yield: 63 mg (58%). d.p. 109  $^{\circ}\text{C}.$  Crystals for X-ray diffraction studies were grown by vapor diffusion of a dichloromethane solution of 4 into benzene. <sup>1</sup>H NMR (400 MHz, THF- $d_8$ ):  $\delta$  7.82–7.80 (m, 2H), 7.41 (dd, J = 7.5, 1.5 Hz, 1H), 7.32-7.30 (m, 1H), 7.23 (d, J = 7.0 Hz, 1H), 7.03-7.00 (m, 3H), 6.94-6.92 (m, 1H), 6.89-6.84 (m, 1H), 6.83-6.81 (m, 1H), 6.78-6.74 (m, 1H), 6.71 (td, J = 7.5, 1.5 Hz, 1H), 6.58-6.53 (m, 4H), 6.46 (td, J = 7.5, 1.5 Hz, 1H), 6.39 (s, br, 3H), 6.21 (s, br, 1H), 6.16-6.14 (m, 1H), 2.05 (s, 1H), -0.65 (s, 9H);  ${}^{13}C\{{}^{1}H\}$  NMR (101 MHz, THF- $d_8$ ):  $\delta$  154.70, 149.30, 143.78, 140.01, 136.82, 135.94, 131.63, 129.62, 127.28, 126.23, 125.16, 124.74, 124.58, 124.49, 123.32, 123.12, 121.88, 117.97, 1.65; <sup>11</sup>B

NMR (128 MHz, THF- $d_8$ ):  $\delta$  –4.1; FT-IR (cm<sup>-1</sup> (ranked intensity)): 3044 (15), 2951 (13), 1591 (3), 1493 (4), 1425 (10), 1307 (7), 1241 (5), 1174 (11), 1027 (9), 842 (2), 783 (14), 741 (1), 690 (6), 612 (8), 466 (12).

Synthesis of 5. A solution of phenol (42 mg, 0.45 mmol) in THF (1 mL) was added to a solution of A (83 mg, 0.23 mmol) in THF (2 mL) while stirring at room temperature. The resulting solution was transferred to a pressure tube with a Teflon cap and heated at 60 °C for 24 h, after which the volatile components were removed in vacuo. The residue was then washed with 1:1 dichloromethane/n-pentane (2) × 3 mL) and dried in vacuo to yield 5 as a white solid. Yield: 65 mg (75%). d.p. 173 °C. Crystals for X-ray diffraction studies were grown by vapor diffusion of a dichloromethane solution of 5 into hexanes. <sup>1</sup>H NMR (400 MHz, CDCl<sub>3</sub>):  $\delta$  7.57 (d, J = 7.5 Hz, 1H), 7.35 (d, J = 7.0 Hz, 1H), 7.29-7.27 (m, 1H), 7.23-7.19 (m, 1H), 7.17-7.14 (m, 1H), 7.08-7.06 (m, 3H), 6.95-6.87 (m, 4H), 6.81 (t, J = 7.5 Hz, 2H), 6.69-6.66 (m, 1H), 6.59 (t, J = 7.5 Hz 1H), 6.42 (d, J = 8.0 Hz, 2H), 2.11-2.07 (m, 1H), 2.00-1.96 (m, 1H);  $^{13}C\{^{1}H\}$  NMR (101 MHz, CDCl<sub>3</sub>):  $\delta$  160.92, 145.38, 139.36, 137.86, 132.98, 131.09, 130.68, 129.24, 127.78, 127.34, 126.97, 126.36, 125.21, 124.83, 124.17, 123.98, 120.44, 118.22;  $^{11}\mathrm{B}$  NMR (128 MHz, CDCl<sub>3</sub>):  $\delta$ -1.5; FT-IR (cm<sup>-1</sup> (ranked intensity)): 3045 (14), 1590 (5), 1486 (2), 1426 (8), 1255 (4), 1167 (9), 1070 (13), 1023 (15), 998 (12), 903 (3), 752 (1), 699 (6), 619 (10), 598 (11), 564 (7).

#### ASSOCIATED CONTENT

## **Supporting Information**

The Supporting Information is available free of charge at https://pubs.acs.org/doi/10.1021/acs.organomet.1c00261.

Multinuclear NMR spectra and FT-IR spectra for 1–5 and X-ray crystallographic and computational details (PDF)

Crystal structure data (XYZ)

## **Accession Codes**

CCDC 2055588–2055593 contain the supplementary crystallographic data for this paper. These data can be obtained free of charge via www.ccdc.cam.ac.uk/data\_request/cif, or by emailing data\_request@ccdc.cam.ac.uk, or by contacting The Cambridge Crystallographic Data Centre, 12 Union Road, Cambridge CB2 1EZ, UK; fax: +44 1223 336033.

## AUTHOR INFORMATION

## **Corresponding Author**

Caleb D. Martin — Department of Chemistry and Biochemistry, Baylor University, Waco, Texas 76798, United States; Orcid.org/0000-0001-9681-0160; Email: caleb\_d\_martin@baylor.edu

#### **Authors**

**Tyler A. Bartholome** – Department of Chemistry and Biochemistry, Baylor University, Waco, Texas 76798, United States

Jesse J. Martinez – Department of Chemistry and Biochemistry, Baylor University, Waco, Texas 76798, United States

Aishvaryadeep Kaur — Department of Chemistry and Physics, La Trobe Institute for Molecular Science, La Trobe University, Melbourne, Victoria 3086, Australia

David J. D. Wilson – Department of Chemistry and Physics, La Trobe Institute for Molecular Science, La Trobe University, Melbourne, Victoria 3086, Australia; orcid.org/0000-0002-0007-4486

Jason L. Dutton – Department of Chemistry and Physics, La Trobe Institute for Molecular Science, La Trobe University, Melbourne, Victoria 3086, Australia; o orcid.org/0000-0002-0361-4441

Complete contact information is available at: https://pubs.acs.org/10.1021/acs.organomet.1c00261

## **Author Contributions**

The manuscript was written through contributions of all authors. All authors have given approval to the final version of the manuscript.

#### **Notes**

The authors declare no competing financial interest.

## ACKNOWLEDGMENTS

We are grateful to the Welch Foundation (Grant No. AA-1846), the National Science Foundation for a CAREER Award (Award No. 1753025), and the ARC (FT17010007 and DP200100013) for their generous support of this work. NCI, Intersect, and La Trobe University are acknowledged for their generous allocations of computing resources. We thank Dr. Kevin K. Klausmeyer for assistance with X-ray crystallography.

## REFERENCES

- (1) Beller, M.; Seayad, J.; Tillack, A.; Jiao, H. Catalytic Markovnikov and anti-Markovnikov Functionalization of Alkenes and Alkynes: Recent Developments and Trends. *Angew. Chem., Int. Ed.* **2004**, *43*, 3368–3398.
- (2) Rodriguez-Ruiz, V.; Carlino, R.; Bezzenine-Lafollée, S.; Gil, R.; Prim, D.; Schulz, E.; Hannedouche, J. Recent developments in alkene hydro-functionalisation promoted by homogeneous catalysts based on earth abundant elements: formation of C-N, C-O and C-P bond. *Dalton Trans.* **2015**, *44*, 12029–12059.
- (3) Liu, C.; Bender, C. F.; Han, X.; Widenhoefer, R. A. Platinum-catalyzed hydrofunctionalization of unactivated alkenes with carbon, nitrogen and oxygen nucleophiles. *Chem. Commun.* **2007**, 3607–3618.
- (4) Chen, J.; Lu, Z. Asymmetric hydrofunctionalization of minimally functionalized alkenes *via* earth abundant transition metal catalysis. *Org. Chem. Front.* **2018**, *5*, 260–272.
- (5) Obligacion, J. V.; Chirik, P. J. Earth-abundant transition metal catalysts for alkene hydrosilylation and hydroboration. *Nat. Rev. Chem.* **2018**, *2*, 15–34.
- (6) Li, G.; Huo, X.; Jiang, X.; Zhang, W. Asymmetric synthesis of allylic compounds *via* hydrofunctionalisation and difunctionalisation of dienes, allenes, and alkynes. *Chem. Soc. Rev.* **2020**, 49, 2060–2118.
- (7) Wang, X.-X.; Lu, X.; Li, Y.; Wang, J.-W.; Fu, Y. Recent advances in nickel-catalyzed reductive hydroalkylation and hydroarylation of electronically unbiased alkenes. *Sci. China: Chem.* **2020**, *63*, 1586–1600.
- (8) Burgess, K.; Ohlmeyer, M. J. Transition-Metal-Promoted Hydroborations of Alkenes, Emerging Methodology for Organic Transformations. *Chem. Rev.* **1991**, *91*, 1179–1191.
- (9) Tamang, S. R.; Bedi, D.; Shafiei-Haghighi, S.; Smith, C. R.; Crawford, C.; Findlater, M. Cobalt-Catalyzed Hydroboration of Alkenes, Aldehydes, and Ketones. *Org. Lett.* **2018**, *20*, 6695–6700.
- (10) Bismuto, A.; Cowley, M. J.; Thomas, S. P. Aluminum-Catalyzed Hydroboration of Alkenes. *ACS Catal.* **2018**, *8*, 2001–2005.
- (11) Beletskaya, I.; Pelter, A. Hydroborations Catalysed by Transition Metal Complexes. *Tetrahedron* **1997**, *53*, 4957–5026.
- (12) Thomas, S. P.; Aggarwal, V. K. Asymmetric Hydroboration of 1,1-Disubstituted Alkenes. *Angew. Chem., Int. Ed.* **2009**, 48, 1896–1898.
- (13) Tamang, S. R.; Findlater, M. Emergence and Applications of Base Metals (Fe, Co, and Ni) in Hydroboration and Hydrosilylation. *Molecules* **2019**, 24, 3194.
- (14) DiBenedetto, T. A.; Parsons, A. M.; Jones, W. D. Markovnikov-Selective Hydroboration of Olefins Catalyzed by a Copper N-

- Heterocyclic Carbene Complex. *Organometallics* **2019**, 38, 3322–3326.
- (15) Bosnich, B. Asymmetric Catalysis. A Comparative Study of the Mechanisms of Intramolecular Hydroacylation and Hydrosilation. *Acc. Chem. Res.* **1998**, *31*, 667–674.
- (16) Pérez, M.; Hounjet, L. J.; Caputo, C. B.; Dobrovetsky, R.; Stephan, D. W. Olefin Isomerization and Hydrosilylation Catalysis by Lewis Acidic Organofluorophosphonium Salts. *J. Am. Chem. Soc.* **2013**, *135*, 18308–18310.
- (17) Andrews, R. J.; Chitnis, S. S.; Stephan, D. W. Carbonyl and olefin hydrosilylation mediated by an air-stable phosphorus(III) dication under mild conditions. *Chem. Commun.* **2019**, *55*, 5599–5602.
- (18) Du, X.; Huang, Z. Advances in Base-Metal-Catalyzed Alkene Hydrosilylation. ACS Catal. 2017, 7, 1227–1243.
- (19) Müller, T. E.; Beller, M. Metal-Initiated Amination of Alkenes and Alkynes. *Chem. Rev.* **1998**, *98*, *675*–703.
- (20) Huang, L.; Arndt, M.; Gooßen, K.; Heydt, H.; Gooßen, L. J. Late Transition Metal-Catalyzed Hydroamination and Hydroamidation. *Chem. Rev.* **2015**, *115*, 2596–2697.
- (21) Streiff, S.; Jérôme, F. Hydroamination of non-activated alkenes with ammonia: a holy grail in catalysis. *Chem. Soc. Rev.* **2021**, *50*, 1512–1521.
- (22) Hannedouche, J.; Schulz, E. Asymmetric Hydroamination: A Survey of the Most Recent Developments. *Chem. Eur. J.* **2013**, *19*, 4972–4985.
- (23) Barreiro, E. M.; Adrio, L. A.; Hii, K. K. M.; Brazier, J. B. Coinage Metal Catalysts for the Addition of O-H to C = C Bonds. *Eur. J. Org. Chem.* **2013**, 2013, 1027–1039.
- (24) Xie, W.-B.; Li, Z. Asymmetric Synthesis of Ethers by Catalytic Alkene Hydroalkoxylation. *Synthesis* **2020**, *52*, 2127–2146.
- (25) Willis, M. C. Transition Metal Catalyzed Alkene and Alkyne Hydroacylation. *Chem. Rev.* **2010**, *110*, 725–748.
- (26) Pei, T.; Widenhoefer, R. A. Palladium-Catalyzed Intramolecular Addition of 1,3-Diones to Unactivated Olefins. *J. Am. Chem. Soc.* **2001**, *123*, 11290–11291.
- (27) DiRocco, D. A.; Rovis, T. Organocatalytic Hydroacylation of Unactivated Alkenes. *Angew. Chem., Int. Ed.* **2011**, *50*, 7982–7983.
- (28) Murphy, S. K.; Dong, V. M. Enantioselective hydroacylation of olefins with rhodium catalysts. *Chem. Commun.* **2014**, *50*, 13645–13649.
- (29) Ruiz Espelt, L.; Wiensch, E. M.; Yoon, T. P. Brønsted Acid Cocatalysts in Photocatalytic Radical Addition of  $\alpha$ -Amino C-H Bonds across Michael Acceptors. *J. Org. Chem.* **2013**, *78*, 4107–4114.
- (30) Chen, X.; Rao, W.; Yang, T.; Koh, M. J. Alkyl halides as both hydride and alkyl sources in catalytic regioselective reductive olefin hydroalkylation. *Nat. Commun.* **2020**, *11*, 5857.
- (31) Andreatta, J. R.; McKeown, B. A.; Gunnoe, T. B. Transition metal catalyzed hydroarylation of olefins using unactivated substrates: Recent developments and challenges. *J. Organomet. Chem.* **2011**, 696, 305–315.
- (32) Wang, Z.-X.; Bai, X.-Y.; Li, B.-J. Recent Progress of Transition-Metal-Catalyzed Enantioselective Hydroalkynylation of Alkenes. *Synlett* **2017**, 28, 509–514.
- (33) Shirakura, M.; Suginome, M. Nickel-Catalyzed Regioselective Hydroalkynylation of Styrenes: Improved Catalyst System, Reaction Scope, and Mechanism. *Org. Lett.* **2009**, *11*, 523–526.
- (34) Bai, X.-Y.; Wang, Z.-X.; Li, B.-J. Iridium-Catalyzed Enantioselective Hydroalkynylation of Enamides for the Synthesis of Homopropargyl Amides. *Angew. Chem., Int. Ed.* **2016**, *55*, 9007–9011.
- (35) Fan, B.-M.; Yang, Q.-j.; Hu, J.; Fan, C.-l.; Li, S.-f.; Yu, L.; Huang, C.; Tsang, W. W.; Kwong, F. Y. Asymmetric Hydroalkynylation of Norbornadienes Promoted by Chiral Iridium Catalysts. *Angew. Chem., Int. Ed.* **2012**, *51*, 7821–7824.
- (36) Braunschweig, H.; Hörl, C. Unexpected cluster formation upon hydroboration of a neutral diborene with 9-BBN. *Chem. Commun.* **2014**, *50*, 10983–10985.

- (37) Brückner, T.; Heß, M.; Stennett, T. E.; Rempel, A.; Braunschweig, H. Synthesis of Boron Analogues of Enamines via Hydroamination of a Boron-Boron Triple Bond. *Angew. Chem., Int. Ed.* **2021**, *60*, 736–741.
- (38) Brückner, T.; Stennett, T. E.; Heß, M.; Braunschweig, H. Single and Double Hydroboration of B-B Triple Bonds and Convergent Routes to a Cationic Tetraborane. *J. Am. Chem. Soc.* **2019**, *141*, 14898–14903.
- (39) Stennett, T. E.; Jayaraman, A.; Brückner, T.; Schneider, L.; Braunschweig, H. Hydrophosphination of boron-boron multiple bonds. *Chem. Sci.* **2020**, *11*, 1335–1341.
- (40) Braunschweig, H.; Dewhurst, R. D.; Hörl, C.; Phukan, A. K.; Pinzner, F.; Ullrich, S. Direct Hydroboration of B = B Bonds: A Mild Strategy for the Proliferation of B-B Bonds. *Angew. Chem., Int. Ed.* **2014**, *53*, 3241–3244.
- (41) Hoefelmeyer, J. D.; Solé, S.; Gabbaï, F. P. Reactivity of the dimesityl-1,8-naphthalenediylborate anion: isolation of the borataal-kene isomer and synthesis of 1,8-diborylnaphthalenes. *Dalton Trans.* **2004**, 1254–1258.
- (42) Bauer, J.; Braunschweig, H.; Hörl, C.; Radacki, K.; Wahler, J. Synthesis of Zwitterionic Cobaltocenium Borate and Borata-alkene Derivatives from a Borole-Radical Anion. *Chem. Eur. J.* **2013**, *19*, 13396–13401.
- (43) Rathke, M. W.; Kow, R. Generation of Boron-Stabilized Carbanions. J. Am. Chem. Soc. 1972, 94, 6854–6856.
- (44) Pelter, A. Some chemistry of hindered organoboranes. *Pure Appl. Chem.* **1994**, *66*, 223–233.
- (45) Pardasani, R. T. Studies on the Synthesis and Properties of Boron Stabilised Carbanions. J. Indian Chem. Soc. 1997, 74, 433-439.
- (46) Pelter, A.; Williams, L.; Wilson, J. W. The Dimesitylboron Group in Organic Synthesis 2. The C-Alkylation of Alkyldimesitylboranes. *Tetrahedron Lett.* **1983**, *24*, 627–630.
- (47) Pelter, A.; Warren, L.; Wilson, J. W. Hindered Organoboron Groups in Organic Chemistry. 20. Alkylations and Acylations of Dimesitylboron Stabilised Carbanions. *Tetrahedron* **1993**, 49 (14), 2888–3006.
- (48) Pelter, A.; Vaughan-Williams, G. F.; Rosser, R. M. Hindered Organoboron Groups in Organic Chemistry. 21. The Reactions of Dimesitylboron Stabilised Carbanions with Oxiranes. *Tetrahedron* 1993, 49, 3007–3034.
- (49) Pelter, A.; Bugden, G.; Rosser, R. The Dimesitylboron Group in Organic Synthesis 8. Preparations of 1,3-Diols from Oxiranes. *Tetrahedron Lett.* **1985**, *26*, 5097–5100.
- (50) Pelter, A.; Singaram, B.; Wilson, J. W. The Dimesitylboron Group in Organic Synthesis. 4. The 'Boron Wittig' Reaction. *Tetrahedron Lett.* **1983**, 24, 635–636.
- (51) Kawashima, T.; Yamashita, N.; Okazaki, R. Synthesis, Structure, and Thermolysis of a Tetracoordinate 1,2-Oxaboretanide: An Intermediate of the Boron-Wittig Reaction under Basic Conditions. *J. Am. Chem. Soc.* **1995**, *117*, 6142–6143.
- (52) Wang, T.; Kohrt, S.; Daniliuc, C. G.; Kehr, G.; Erker, G. Borata-Wittig olefination reactions of ketones, carboxylic esters and amides with bis(pentafluorophenyl)borata-alkene reagents. *Org. Biomol. Chem.* **2017**, *15*, 6223–6232.
- (53) Moquist, P.; Chen, G.-Q.; Mück-Lichtenfeld, C.; Bussmann, K.; Daniliuc, C. G.; Kehr, G.; Erker, G.  $\alpha$ -CH acidity of alkyl-B(C<sub>6</sub>F<sub>5</sub>)<sub>2</sub> compounds the role of stabilized borata-alkene formation in frustrated Lewis pair chemistry. *Chem. Sci.* **2015**, *6*, 816–825.
- (54) Kohrt, S.; Dachwitz, S.; Daniliuc, C. G.; Kehr, G.; Erker, G. Stabilized borata-alkene formation: structural features, reactions and the role of the counter cation. *Dalton Trans.* **2015**, *44*, 21032–21040.
- (55) Wang, T.; Kehr, G.; Liu, L.; Grimme, S.; Daniliuc, C. G.; Erker, G. Selective Oxidation of an Active Intramolecular Amine/Borane Frustrated Lewis Pair with Dioxygen. *J. Am. Chem. Soc.* **2016**, *138*, 4302–4305.
- (56) Kobayashi, A.; Suzuki, K.; Kitamura, R.; Yamashita, M. Formation of BCBH/BCBCl Four-Membered Rings by Complexation of Boron- and Nitrogen-Substituted Acetylene with Hydro-/Chloroboranes. *Organometallics* **2020**, *39*, 383–387.

- (57) Bartholome, T. A.; Kaur, A.; Wilson, D. J. D.; Dutton, J. L.; Martin, C. D. The 9-Borataphenanthrene Anion. *Angew. Chem., Int. Ed.* **2020**, *59*, 11470–11476.
- (58) A cyclic alkyl amino carbene (CAAC)-borylene adduct that has allenic character and can be described as a B=C bond was shown to undergo hydrogenation with H<sub>2</sub> in the following paper: Dahcheh, F.; Martin, D.; Stephan, D. W.; Bertrand, G. Synthesis and Reactivity of a CAAC-Aminoborylene Adduct: A Hetero-Allene or an Organoboron Isoelectronic with Singlet Carbenes. *Angew. Chem., Int. Ed.* **2014**, *53*, 13159–13163.
- (59) Hitchcock, P. B.; Lappert, M. F.; Liu, D.-S. Transformation of the Bis(trimethylsilyl)methyl into Aza-allyl and  $\beta$ -Diketinimato Ligands; the X-Ray Structures of  $[\text{Li}\{N(R)C(Bu^t)CH(R)\}]_2$  and  $[\text{Zr}\{N(R)C(Bu^t)CHC(Ph)N(R)\}Cl_3](R = SiMe_3)$ . *J. Chem. Soc., Chem. Commun.* **1994**, 2637–2638.
- (60) Hitchcock, P. B.; Lappert, M. F.; Layh, M. Synthesis and structures of tin(II) and lead(II) 1-aza-allyls; the  $[N(SiMe_3)C(Ph)-C(SiMe_3)_2]^-$  ligand. *Inorg. Chim. Acta* **1998**, 269, 181–190.
- (61) While the presence of impurities in the crude product indicates that the occurrence of C–F activation in the reaction with  $C_6F_5H$  cannot be ruled out, compound **2** was found to be the clear major product by  $^1H$ ,  $^{19}F\{^1H\}$ , and  $^{11}B$  NMR spectroscopy.
- (62) Cook, K. S.; Piers, W. E.; McDonald, R. Synthesis and Chemistry of Zwitterionic Tantala-3-boratacyclopentenes: Olefin-like Reactivity of a Borataalkene Ligand. *J. Am. Chem. Soc.* **2002**, *124*, 5411–5418.
- (63) Compound **A** was dissolved in THF, 1,4-dioxane, and dimethoxyethane and showed no reaction at room temperature over 24 h. THF solutions of **A** did not show any signs of reaction with  $H_2$  and 2,3,4,5,6-pentafluorotoluene at room temperature over 24 h.
- (64) Matthews, W. S.; Bares, J. E.; Bartmess, J. E.; Bordwell, F. G.; Cornforth, F. J.; Drucker, G. E.; Margolin, Z.; McCallum, R. J.; McCollum, G. J.; Vanier, N. R. Equilibrium Acidities of Carbon Acids. VI. Establishment of an Absolute Scale of Acidities in Dimethyl Sulfoxide Solution. J. Am. Chem. Soc. 1975, 97, 7006–7014.
- (65) Bordwell, F. G.; Branca, J. C.; Hughes, D. L.; Olmstead, W. N. Equilibria Involving Organic Anions in Dimethyl Sulfoxide and *N*-Methylpyrrolidin-2-one: Acidities, Ion Pairing, and Hydrogen Bonding. *J. Org. Chem.* **1980**, *45*, 3305–3313.
- (66) Olmstead, W. N.; Margolin, Z.; Bordwell, F. G. Acidities of Water and Simple Alcohols in Dimethyl Sulfoxide Solution. *J. Org. Chem.* **1980**, *45*, 3295–3299.
- (67) Bordwell, F. G.; McCallum, R. J.; Olmstead, W. N. Acidities and Hydrogen Bonding of Phenols in Dimethyl Sulfoxide. *J. Org. Chem.* **1984**, *49*, 1424–1427.
- (68) Bordwell, F. G.; Drucker, G. E.; Andersen, N. H.; Denniston, A. D. Acidities of Hydrocarbons and Sulfur-Containing Hydrocarbons in Dimethyl Sulfoxide Solution. *J. Am. Chem. Soc.* **1986**, *108*, 7310–7313
- (69) Shen, K.; Fu, Y.; Li, J.-N.; Liu, L.; Guo, Q.-X. What are the pK<sub>a</sub> values of C-H bonds in aromatic heterocyclic compounds in DMSO? *Tetrahedron* **2007**, *63*, 1568–1576.
- (70) Sheldrick, G. M. A short history of SHELX. Acta Crystallogr., Sect. A: Found. Crystallogr. 2008, A64, 112–122.
- (71) Dolomanov, O. V.; Bourhis, L. J.; Gildea, R. J.; Howard, J. A. K.; Puschmann, H. OLEX2: a complete structure solution, refinement and analysis program. *J. Appl. Crystallogr.* **2009**, 42, 339–341.
- (72) Lee, C.; Yang, W.; Parr, R. G. Development of the Colle-Salvetti correlation-energy formula into a functional of the electron density. *Phys. Rev. B: Condens. Matter Mater. Phys.* **1988**, 37, 785–789.
- (73) Becke, A. D. Density-functional thermochemistry. III. The role of exact exchange. *J. Chem. Phys.* **1993**, *98*, 5648–5652.
- (74) Becke, A. D. A new mixing of Hartree-Fock and local density-functional theories. *J. Chem. Phys.* **1993**, 98, 1372–1377.
- (75) Grimme, S.; Antony, J.; Ehrlich, S.; Krieg, H. A consistent and accurate ab initio parametrization of density functional dispersion correction (DFT-D) for the 94 elements H-Pu. *J. Chem. Phys.* **2010**, 132, 154104.

- (76) Grimme, S.; Ehrlich, S.; Goerigk, L. Effect of the damping function in dispersion corrected density functional theory. *J. Comput. Chem.* **2011**, 32, 1456–1465.
- (77) Weigend, F.; Ahlrichs, R. Balanced basis sets of split valence, triple zeta valence and quadruple zeta valence quality for H to Rn: Design and assessment of accuracy. *Phys. Chem. Chem. Phys.* **2005**, *7*, 3297–3305.
- (78) Marenich, A. V.; Cramer, C. J.; Truhlar, D. G. Universal Solvation Model Based on Solute Electron Density and on a Continuum Model of the Solvent Defined by the Bulk Dielectric Constant and Atomic Surface Tensions. *J. Phys. Chem. B* **2009**, *113*, 6378–6396.
- (79) Frisch, M. J.; Trucks, G. W.; Schlegel, H. B.; Scuseria, G. E.; Robb, M. A.; Cheeseman, J. R.; Scalmani, G.; Barone, V.; Petersson, G. A.; Nakatsuji, H.; Li, X.; Caricato, M.; Marenich, A. V.; Bloino, J.; Janesko, B. G.; Gomperts, R.; Mennucci, B.; Hratchian, H. P.; Ortiz, J. V.; Izmaylov, A. F.; Sonnenberg, J. L.; Williams-Young, D.; Ding, F.; Lipparini, F.; Egidi, F.; Goings, J.; Peng, B.; Petrone, A.; Henderson, T.; Ranasinghe, D.; Zakrzewski, V. G.; Gao, J.; Rega, N.; Zheng, G.; Liang, W.; Hada, M.; Ehara, M.; Toyota, K.; Fukuda, R.; Hasegawa, J.; Ishida, M.; Nakajima, T.; Honda, Y.; Kitao, O.; Nakai, H.; Vreven, T.; Throssell, K.; Montgomery, J. A., Jr.; Peralta, J. E.; Ogliaro, F.; Bearpark, M. I.; Heyd, J. J.; Brothers, E. N.; Kudin, K. N.; Staroverov, V. N.; Keith, T. A.; Kobayashi, R.; Normand, J.; Raghavachari, K.; Rendell, A. P.; Burant, J. C.; Iyengar, S. S.; Tomasi, J.; Cossi, M.; Millam, J. M.; Klene, M.; Adamo, C.; Cammi, R.; Ochterski, J. W.; Martin, R. L.; Morokuma, K.; Farkas, O.; Foresman, J. B.; Fox, D. J. Gaussian 16, Rev. C.01; Wallingford, CT, 2016.
- (80) Marenich, A. V.; Jerome, S. V.; Cramer, C. J.; Truhlar, D. G. Charge Model 5: An Extension of Hirshfeld Population Analysis for the Accurate Description of Molecular Interactions in Gaseous and Condensed Phases. J. Chem. Theory Comput. 2012, 8, 527–541.
- (81) Chai, J.-D.; Head-Gordon, M. Long-range corrected hybrid density functionals with damped atom-atom dispersion corrections. *Phys. Chem. Phys.* **2008**, *10*, 6615–6620.